Cancer Immunology, Immunotherapy (2023) 72:3243–3257
https://doi.org/10.1007/s00262-023-03490-8

RESEARCH

Chimeric antigen receptor macrophages activated through TLR4 or IFN-γ receptors suppress breast cancer growth by targeting VEGFR2

Zhaojun Duan[1] · Zhen Li[1] · Ziyuan Wang[1] · Chong Chen[1] · Yunping Luo[1]

Received: 22 January 2023 / Accepted: 28 June 2023 / Published online: 12 July 2023

Abstract

Chimeric antigen receptor macrophage (CAR-M) is a promising immunotherapy strategy of anti-tumor due to its high infiltration, direct phagocytosis of tumor cells, immunomodulation of tumor microenvironment (TME) and linkage of innate and adaptive immunity. Here a series of novelly designed CAR-Ms by targeting vascular endothelial growth factor receptor-2 (VEGFR2), which highly expressed in tumor cells and TME, were evaluated. Their activation signals were transduced by Tlr4 or Ifn-γ receptors either alone or in combination, which were designed to mediate M1 polarization of macrophages as the downstream of lipopolysaccharide or Ifn-γ that had been widely reported. Our results showed that VEGFR2-targeting CAR-Ms could be activated under the stimulation of VEGFR2-expressing cells. They exhibited higher expression of CD86, MHCII and TNF-α in vitro and enhanced tumor suppressive abilities in vivo. Implantation of these CAR-Ms into 4T1 breast cancer-bearing mice could obviously inhibit the progression of tumor without significant toxic side effects, especially the group of mmC in which constructed with Tlr4 as the intracellular domain of CAR. In conclusion, this research provides a promising design of CAR that induce macrophages activation by Tlr4 and/or Ifn-γ receptors, and these CAR-Ms could effectively inhibit tumor growth through targeting VEGFR2.

Keywords CAR-M · VEGFR2 · Tlr4 · Ifngr1 · Ifngr2 · Breast cancer

Introduction

As the most representative adoptive cell transfer therapy for cancer, chimeric antigen receptor T-cell (CAR-T) has achieved remarkable clinical success in the treatment of hematologic malignancies [1]. Eight CAR-T products targeting CD19 or B-cell maturation antigens (BCMA) have been approved for the treatment of B-cell malignancies globally. However, CAR-T therapy has encountered many challenges in the treatment of solid tumors [2], such as the difficulty in effective infiltration into solid tumors, the inactivation in the immunosuppressive tumor microenvironment (TME) and the severe side effects that often accompany CAR-T therapy [3, 4]. These have led to a lack of exciting outcomes of CAR-T in the treatment of solid tumors, even with strong preclinical studies.

Then CAR-macrophages emerged as a promising strategy [5–8]. Macrophages possess many advantages over T cells, including trafficking and infiltration into TME, direct phagocytosis of tumor cells, and modulation of immunosuppressive TME [9]. Generally, macrophages can be broadly classified into two major categories, the classically activated M1 pro-inflammatory macrophages induced by lipopolysaccharide (LPS) or interferon-gamma (IFN-γ) and alternatively activated M2 anti-inflammatory macrophages induced by IL-4 or IL-13 [10]. Once LPS binds to Toll-like receptor 4 (TLR4) on the surface of macrophages, the activation signal is transmitted to the Toll/IL-1R homology (TIR) region, which further activates the NF-κB and MAPKs signaling pathways [11, 12]. IFN-γ binds to interferon gamma receptor 1 (IFNGR1) and IFNGR2 to form a complex followed by phosphorylating the receptor complex and activating the MAPKs, PI3K-AkT and NF-κB pathways, ultimately leading to the release of various pro-inflammatory cytokines [13–15]. Pro-inflammatory cytokines secreted by

Zhaojun Duan and Zhen Li contributed equally in this work.

✉ Yunping Luo
ypluo@ibms.pumc.edu.cn

[1] Department of Immunology, Institute of Basic Medical Sciences, Chinese Academy of Medical Sciences, School of Basic Medicine, Peking Union Medical College, Beijing 100005, China

M1 macrophages includes tumor necrosis factor-α (TNF-α) and IL-6 [9]. M2 macrophages are mainly involved in the clearance of parasites and maintenance of homeostasis by secreting cytokines such as IL-10, PGE2 and TGF-β [9]. Tumor associated macrophages (TAMs), often thought of as M2-like macrophages, are widely considered to suppress endogenous antitumor immunity in TME [16]. Numerous publications have reported that M2-type TAMs are directly or indirectly involved in several key processes associated with malignancy development, including tumor angiogenesis, tumor invasion and metastasis, regulation of TME and tumor treatment resistance [9, 17, 18]. Unlike the low infiltration of T cells, macrophages infiltrate up to 30–50% of all immune cells in a variety of solid tumors [19]. In fact, tumor cells recruit monocytes from peripheral circulating blood into the TME by secreting chemokines such as CSF-1, VEGF and CCL2, and then domesticate them into TAMs that promote tumor growth [20]. A larger number of TAMs in tumor often indicates a higher tumor grade and a worse prognosis [17]. Hence, blocking the polarization of macrophages recruited into TME toward M2 phenotype or promoting the conversion of suppressive macrophage into pro-inflammatory macrophage through CAR could offer a promising strategy for improving the outcome of tumor immunotherapy [21, 22].

For a majority of tumors, angiogenesis is essential for tumor growth and metastasis [23, 24]. Among all cytokines that induce angiogenesis, VEGF is the most potent and specific one [24, 25]. When the oxygen required for tumor metabolism is insufficient, the expression of VEGF is upregulated, and it binds to vascular endothelial growth factor receptor 2 (VEGFR2) expressed by adjacent vascular endothelial cells to initiate angiogenesis [26, 27]. VEGFR2 plays a critical role in the regulation of angiogenesis, vascular development, and modulation of vascular permeability [28, 29]. The feature that tumor cells require large amounts of oxygen and nutrients to maintain their hypermetabolic state leads to upregulation of VEGFR2 expression in the vascular endothelium in many tumor types [30]. When VEGFR2 is deficient, angiogenesis is inhibited [31]. It has been reported that the combination of VEGFR2 inhibitors and anti-cancer drugs can synergistically kill tumors [24]. Specifically, inhibitors targeting VEGFR2 obtained remarkable achievements in the treatment of breast cancer [32]. This above suggests that VEGFR2 can be a good target in more than one type of tumor.

Thus, we have designed a family of chimeric antigen receptor macrophages (CAR-Ms) targeting VEGFR2. The design aims to promote and maintain the polarization of modified macrophages toward the M1 type. It consists of a single-chain variable fragment (scFv) of anti-VEGFR2 monoclonal antibody in the extracellular domain and an intracellular segment of Tlr4, Ifngr1, Ifngr1 alone or in combination in the intracellular domain, linking by the hinge and transmembrane region of the nearest gene in the intracellular domain. 4T1 murine breast cancer cells and mice models are used to evaluate these VEGFR2-targeting CAR-Ms. The results demonstrated that among all these CAR-Ms, the one with signal transduction through intracellular Tlr4 could elicit secretion of TNF-α and exert consistently obvious antitumor effect both in vitro and in vivo.

Materials and methods

Cell lines

Mouse breast cancer cell lines 4T1, 4T1 labeled with luciferase (4T1-luc) and leukemic macrophage cell line RAW264.7 were gifted by Dr. R. A. Reisfeld (The Scripps Institute, La Jolla, CA). They were cultured in RPMI1640 (Gibco, USA) or DMEM (Gibco, USA) medium supplemented with 10% fetal bovine serum (FBS) (Gibco, USA) and 1% antibiotics (100 U/mL penicillin–0.1 mg/mL streptomycin) (Gibco, USA). Human umbilical vein vascular endothelial cell line HUVEC and embryonic kidney cell line HEK293T were obtained from Prof. Rong Xiang (Nankai University) in 2020. Mouse liver cancer cell line Hepa1-6 was purchased from the Cell Resource Center, Peking Union Medical College.

Animals Studies

Female Balb/c and nude mice, 6–8 weeks of age, were purchased from the Experimental Animal Center of Institute of Basic Medical Sciences of Peking Union Medical College and raised in specific-pathogen-free environment. All experiments involving animals were approved by the Institute Research Ethics Committee of Peking Union Medical College and carried out under the guidelines on laboratory animals. 5×10^5 4T1-luc cells in 100 µl PBS were injected into the mammary fat pads of Balb/c mice. Five days later, all tumor-bearing mice were randomly divided into seven treatment groups (PBS, ctrl (macrophages transfected with empty plasmid), mmA, mmB, mmC, mmD, mmE) with 5 mice in each group. 1×10^6 CAR-Ms in 200 µl PBS or PBS only were injected intravenously (i.v.) on day 6, 12 and 18. Biofluorescence were recorded on day 5 and 20. The process in evaluation using 4T1 cells or nude mice was similar. Tumor volume was calculated by $[(\text{length} \times \text{width}^2)/2]$ and mice weight were measured every other day starting from day 5. The mice were humanely euthanized on day 21. Tumor tissue and organs of the mice were isolated and weighed.

Design of CAR constructs

The scfv of CAR was designed from human VEGFR2 antibody (Ramucirumab) or mouse Vegfr2 antibody (DC101). The intracellular domain of CAR consisted of a single or combination of the following three elements: the intracellular segment of Tlr4 (Gene ID: 21898) containing the TIR domain, the intracellular segment of Ifngr1 (Gene ID: 15979) containing phosphorylation sites that activate downstream signals and bind to other proteins, and the intracellular segment of Ifngr2 (Gene ID: 15980) containing the Fibronectin type-III domain. These elements were connected together with or without a linker (GGGGSGGGGSGGGGS). The hinge and transmembrane region of the nearest gene in the intracellular domain were used as the hinge and transmembrane region of the CAR. An enhanced green fluorescent protein (EGFP) was added after the coding sequence (CDS) of CAR with an internal ribosome entry site (IRES). Finally, the sequences were synthesized by Sangon Biotech (Shanghai) Co., Ltd and inserted into the lentiviral vector Plenti-CMV-EGFP-Puro (gifted by Jianguo Wu, Jinan University) by genetic homologous recombination.

Preparation of CAR-M

The CAR-vector based on Plenti-CMV-CAR-EGFP-Puro plasmid was transfected into HEK293T cell line with packaging plasmids to produce lentivirus. When the density of cultured RAW264.7 cells was about 30–50%, the lentivirus carrying CAR molecules was added. After the infected macrophages grew to high density, the EGFP positive cells were sorted using MA900 (Sony).

Security Assessment

To assess the safety of VEGFR2-targeting CAR-Ms, the CDS of VEGFR2 (Gene ID: 16542) was inserted into the Plenti-CMV-mCherry plasmid, from which the generated lentivirus could express VEGFR2 and mCherry at the same time. Infecting HEK293T cells by the lentivirus to overexpress VEGFR2. CAR-M was co-cultured with VEGFR2-overexpressing HEK293T cells. The percentage of $EGFP^+mCherry^+$ cells in $EGFP^+$ cells was used to analyze the phagocytosis rate.

Western blotting

Total cellular proteins from RAW264.7, HUVEC, 4T1 and Hepa1-6 were obtained using RIPA Lysis Buffer (P0013J, Beyotime) with protease inhibitors (C0001, Topscience). The Pierce BCA assay was used for measuring the protein concentrations. Antibodies against VEGFR2 (9698S, Cell Signaling Technology) and β-actin (20536–1-AP, Proteintech) were used for detection.

Flow cytometry

To evaluate the expression of CAR on the cell membrane, we used a two-step staining protocol: primary stain with human biotinylated VEGFR2 protein (10012-H08H-B, Sino Biological), followed by human TruStain FcX (422302, Biolegend) and secondary stain with PE anti-Biotin (1D4-C5, Biolegend). To assess the phenotype of macrophages, single-cell suspensions were prepared and stained at 4 °C for 30 min with following anti-mouse antibodies: MHCI (AF-88.5), MHCII (M5/114.15.2), CD80 (16-10A1) and CD86 (GL-1). As for evaluating apoptosis of tumor cells, apoptosis detection Kit (62700–80, Biogems) was used. Cells were incubated with APC-Annexin V and anti-mouse CD45 (30-F11) for 30 min at 4 °C and stained with 7-AAD 15 min prior to detection. The frequency or mean fluorescence intensity (MFI) data were acquired by flow cytometry (Millipore, Guava 5HT).

To measure the secretion of TNF-α, GolgiStop (554724, BD Biosciences) was added into the co-culture system. Two hours later, collected cells were incubated with anti-mouse CD45 (30-F11) for 30 min. Then fixation and permeabilization solution (554724, BD Biosciences) were added for 20–30 min. Perforated cells were incubated with anti-mouse TNF-α (MP6-XT22) for 30 min on ice followed by flow cytometry detection. Anti-mouse CD120a (113103, Biolegend) was used to block TNFR according to its manual. The data were analyzed using FlowJo software.

Phagocytosis assay

RAW264.7, HUVEC cells and PKH26 labeled 4T1 cells were co-cultured at a ratio of 1:1:10 in a 5% CO_2, 37 °C incubator. Two hours later, cells were collected and incubated with anti-mouse CD45 antibody at 4 °C for 30 min. The cell subpopulations were detected by flow cytometry within 2 h and the phagocytosis ratio was calculated according to the formula of $(CD45^+PKH26^+)/CD45^+$.

Enzyme-linked immuosorbent assay (ELISA)

TNF-α, IL-6 and IL-1β were quantified by ELISA Kit (Multi Sciences) according to the manufacturer's protocol. Briefly, after the tetramethylbenzidine substrate was fully developed, the OD values at 450 nm and 570 nm were measured within 30 min after the addition of the termination solution. The OD value at 450 nm minus the OD value at 570 nm was used for calibration.

In vivo *imaging*

1 × D-luciferin (E1483, Promega) working fluid was prepared using PBS. Mice bearing 4T1-luc tumor cells were injected intraperitoneally with 200 µl (10 µl/g) of D-luciferin. After 8–10 min, mice were rendered unconscious using isoflurane. Then bioluminescence intensity was captured and analyzed by the in vivo Imaging System (Xenogen IVIS, PerkinElmer).

Immunohistochemical stain (IHC)

Paraffin-embedded tumor tissues were stained after sectioning, dewaxing, hydration, antigen repair and blocking. Antibodies against F4/80 (70076S, CST) and CD31 (GB11063, servicebio) were used for staining.

Statistical analysis

All data were processed using GraphPad Software. Student's t test was used for analyzing the statistical differences between two groups, while one-way ANOVA with Tukey's post-test was used when there were three or more groups. $P < 0.05$ was considered statistically significant.

*, ** or ***, respectively, represents $P < 0.05$, $P < 0.01$ or $P < 0.001$.

Results

Construction of VEGFR2-targeting CAR-M

Our CAR was designed to promote the modified macrophages activation through Tlr4 and/or Ifn-γ receptors. In this research, five kinds of CAR molecules with different structure was constructed and named H/mmA, H/mmB, H/mmC, H/mmD, H/mmE ('H' stands for scFv targeting human VEGFR2 while the first 'm' refers to targeting mouse Vegfr2, the second 'm' is short for macrophages) (Fig. 1a). After infecting RAW264.7 through lentiviral system, the expression of each CAR was evaluated according to the fluorescence intensity of EGFP (Fig. 1a,b) and the surface expression of scFv (Fig. 1c). Their expression patterns were not completely consistent but all of them had an elevated fluorescence intensity of EGFP compared to RAW264.7 itself. Although the CAR-Ms were designed to be activated by VEGFR2-expressing vascular endothelial cells, the phagocytosis rate of HEK293T cells, which was over-expressed with VEGFR2 and mCherry, in the co-culture system with CAR-Ms is less than 0.04%, indicating that VEGFR2-targeting CAR-Ms did not phagocytose non-tumor cells expressing VEGFR2 (Fig. 1d).

VEGFR2-targeting CAR-M cells displayed some M1-like phenotype in co-culture system.

Then the expression of Vegfr2 in several cell lines were detected. The data showed that in comparison with Hepa1-6, 4T1 and RAW264.7, VEGFR2 can only be observed in HUVEC (Fig. 2a). Thus HUVEC cells was predicted to provide the activation signal in the co-culture system with RAW264.7 and PKH26 labeled tumor cells (Fig. 2b). The flow cytometry analysis demonstrated that the antigen-presenting ability of several CAR-Ms could be improved as MHC-II (Fig. 2c) but not MHC-I (Fig. 2d) increased significantly in the groups co-cultured with HmA, HmB, HmC or HmD. Additionally, compared with the unmodified RAW264.7 cells, the expression of CD86 molecules was significantly increased in the groups of HmA, HmB, HmC and HmD (Fig. 2e), although similar tendency did not appear in CD80 (Fig. 2f). Additionally, the M2-like phenotype markers including CD163, CD206, CD36, Arg1 were similar or decreased in the CAR-M groups compared to the ctrl group, except HmB (Fig. S1e–h). But for the M1-like phenotype marker Nos2, the percentage of positive cells was significantly increased in the HmA, HmB, HmC, HmE group (Fig. S1i).

CAR-M cells can be activated by Vegfr2 to secret TNF-α in vitro

To further investigate the phenotype of Vegfr2-targeting CAR-M cells, we examined the expression level of pro-inflammatory cytokine. M1 polarization stimulated by LPS or IFN-γ could result in the activation of NF-κB pathway, which induces the expression of pro-inflammatory cytokines TNF-α, IL-1β and IL-6 [9]. So the supernatant of macrophages alone or co-cultured with tumor cells were divided to detect these three cytokines. Compared to the control (RAW264.7 cells transfected with empty plasmid), mmC and mmD could produce more TNF-α whether co-cultured with 4T1 cells or not (Fig. 3a). It is noteworthy that whether co-cultured with tumor cells or not, the amount of TNF-α generated by macrophages were less than 100 pg/ml. CAR-Ms alone hardly secreted IL-6 (Fig. 3b). After co-culturing with 4T1, IL-6 in co-culture supernatant, especially in mmD and mmE group, were significantly increased (Fig. 3b). However, the concentration of IL-1β in the supernatant is below the range of detection (data not shown).

According to the conception of CAR design, CAR-Ms are supposed to be activated by VEGFR2. The pro-inflammatory cytokines were further detected after adding vascular endothelial cells into the co-culture system. As expected,

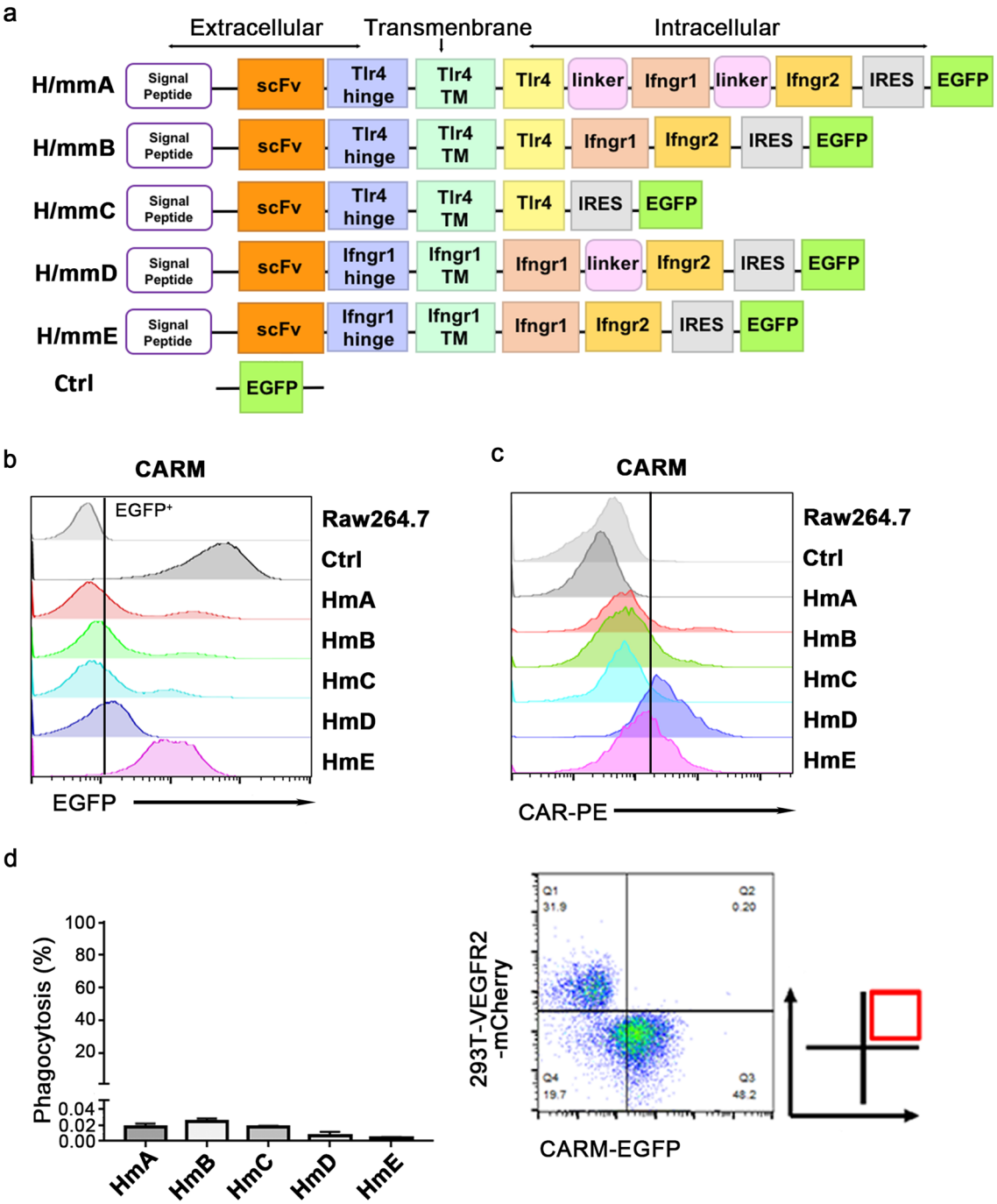

Fig.1 Construction and safety analysis of VEGFR2-targeting CAR-M cells. **a** Schematic diagram of CAR constructs. **b-c** The transfection efficiency of VEGFR2-targeting CAR-M cells was tested by detecting EGFP or scFv of CAR using flow cytometry. **d** Phagocytosis assay in co-culture system of VEGFR2-targeting CAR-M cells and HEK293T cells overexpressing VEGRR2-mCherry at an effector-to-target (E/T) ratio of 1:1 for 2 h. Data imply three independent repeats

when HUVEC cells were added, the secretion of TNF-α increased almost tenfold in all groups (Fig. 4a,b). Notably, TNF-α released by HmC and HmD (Fig. 4a,b) were consistently higher than control whether 4T1 cells were added or not, which indicated that the elevation of their TNF-α were mainly elicited by VEGFR2-expressing HUVEC but not tumor cells. This experiment was repeated using 293 T-mcs cells to simulate HUVEC-VEGFR2-KO cells and 293 T-VEGFR2-mcherry cells instead of HVUEC. Then the supernatant was collected to detect the level of TNF-α. As shown in Fig. S1k, compared to the group co-cultured with 293 T-mcs + 4T1 cells, the secretion of TNF-α

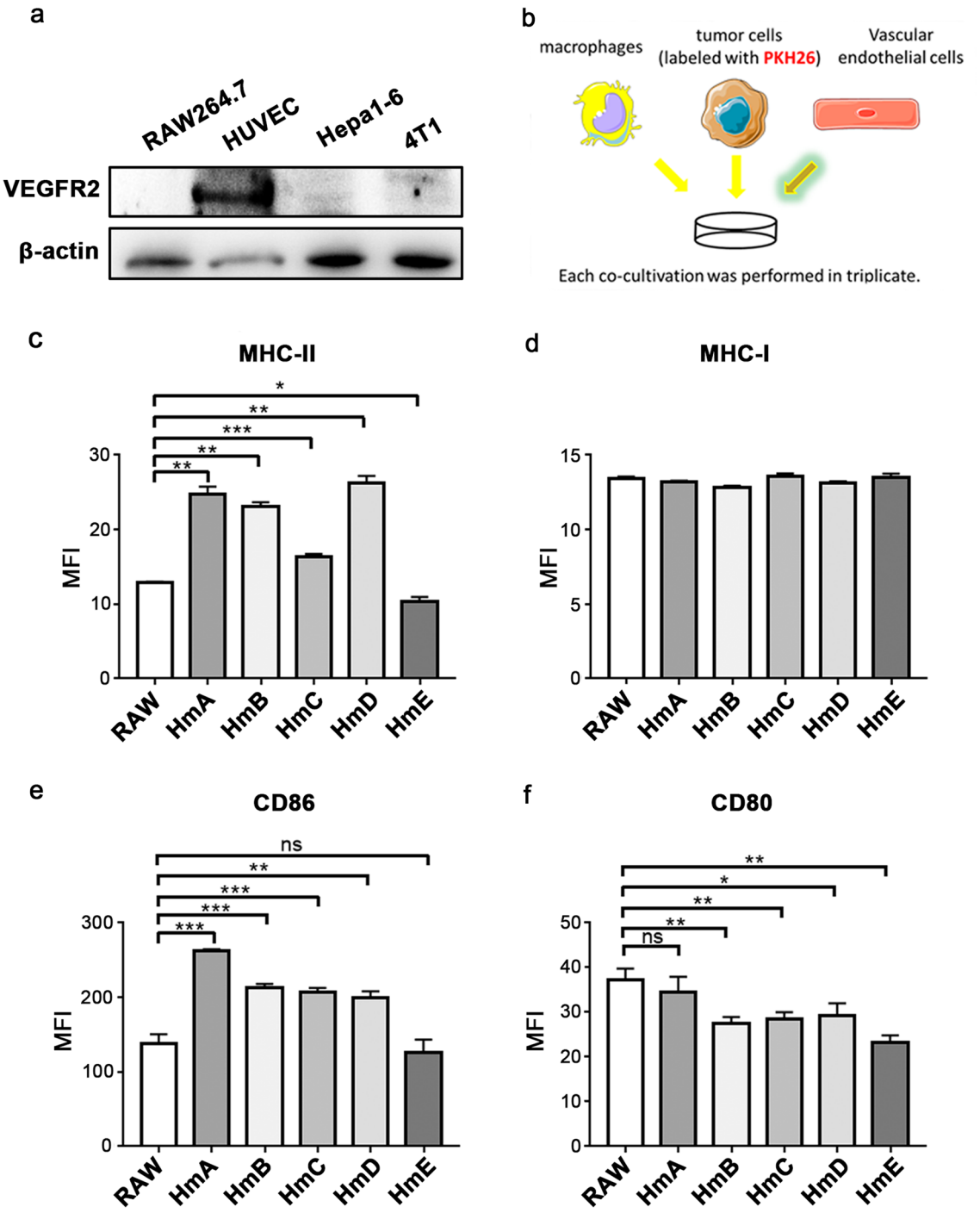

Fig.2 VEGFR2-targeting CAR-M cells displayed some M1-like phenotype in co-culture system. **a** Detecting the expression of VEGFR2 in RAW264.7, HUVEC, Hepa1-6 and 4T1 by western blotting. **b** The co-culture system consists of CAR-Ms, HUVEC cells and PKH26 labeled 4T1 cells at a ratio of 1:1:10. **c, d, e, f** Expression of MHC-II, MHC-I, CD86 and CD80 on CAR-Ms after co-culture. Data represent 3 independent repeats. ns: not significant, $*P<0.05$, $**P<0.01$, $***P<0.001$

was still significantly increased in HmC group co-cultured with 293 T-VEGFR2 + 4T1 cells. Meanwhile, TNF-α in macrophages was also detected by flow cytometry. Upon co-culturing with HUVEC, the percentages of TNF-α^+ cells in HmA, HmB, HmC and HmD were higher than control (Fig. 4c). After the addition of 4T1 cells, although the percentages of TNF-α^+ cells in HmA, HmB, HmC, HmD were still higher than control, the percentages in HmA, HmB,

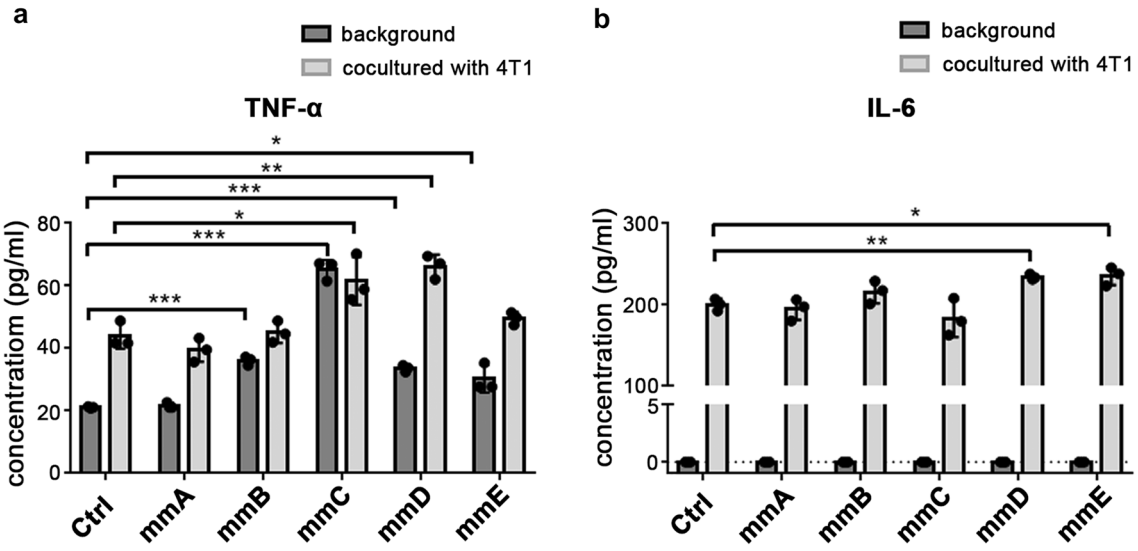

Fig.3 CAR-M cells showed increased expression of pro-inflammatory factor. **a** Secretion of TNF-α in supernatant of CAR-Ms alone and CAR-Ms co-cultured with 4T1. **b** Secretion of IL-6 in supernatant of CAR-Ms alone and CAR-Ms co-cultured with 4T1. *$P < 0.05$, *** $P < 0.001$

HmD and control decreased significantly, except HmC (Fig. 4d). The results suggested that CAR-Ms, especially mmC/HmC, could be activated by VEGFR2-exprssing HUVEC to generate more TNF-α. This activation won't be inhibited even in the presence of tumor derived inhibitory signals.

The VEGFR2-targeting CAR-M cells promoted apoptosis or phagocytosis in vitro

Since apoptosis is a typical outcome of the activation of caspases and JNK signaling pathways caused by TNF-α [33], apoptosis assay was performed based on the CAR-Ms, HUVEC, 4T1 co-culture system. The proportion of early apoptosis (AnnexinV^{+}7-AAD^{-}/CD45^{-}PKH26^{+}) in HmB, HmC or HmD group was significantly increased (Fig. 4e). When blocking TNFR using anti-TNFR in the co-culture system, the differences of early apoptosis rate between the CAR-M groups and the RAW264.7 group disappeared or become reversed (Fig. S1j). Without HUVEC, no statistical difference in the early apoptosis rate of 4T1 cells can be observed between CAR-M and control group (Fig. S1l). Futhermore, the phagocytic ability of CAR-Ms were compared and the results showed that HmA, HmB, and HmD were able to phagocytose more tumor cells (Fig. 4f). It has been reported that M1 polarization stimulated by LPS may result in impaired phagocytosis [34, 35]. Given that the intracellular domain of HmC is Tlr4, which is responsible for delivering the signal of LPS, our results suggested that HmC may inhibit tumors through secreting pro-inflammatory cytokines and promoting apoptosis but not phagocytozing tumor cells directly.

The preliminary validation of the anti-tumor effect of VEGFR2-targeting CAR-M cells in vivo

CAR-M cells were further evaluated in breast cancer mice model. 4T1 cells expressing luciferase were inoculated into the mammary fat pad of 6-week Balb/c mice six days prior to CAR-M cells injection. Bioluminescence images were taken at day 5 and day 20 and CAR-Ms were transferred at day 6, day 12 and day 18 (Fig. 5a). The mice injected with macrophages transfected with empty plasmid or PBS were used as control. Before administration of CAR-Ms, on day 5, the bioluminescence intensity of tumors in group mmA and mmB was significantly higher than control groups, whereas there were no significant difference in other groups (Fig. 5b,c). However, on day 20, when three times of injection of CAR-Ms have been completed, the bioluminescence intensity of tumors in groups mmA, mmB and mmC was obviously diminished (Fig. 5b,d). As for the ratio of intensity on day 20 to that on day 5, it was significantly lower after administrating mmA, mmB, mmC or mmD (Fig. 5e). This experiment demonstrated that administration of mmA, mmB, mmC and mmD for mice with breast cancer could inhibit the growth of tumor. Considering that the developments of tumors in two control groups were similar, the group of treatment with PBS in subsequent experiments was used as control (Fig. 5e).

The mmB and mmC demonstrated powerful antitumor effects in immunocompetent mice

Then the antitumor effects of CAR-M cells were validated again in immunocompetent mice bearing 4T1 cells without

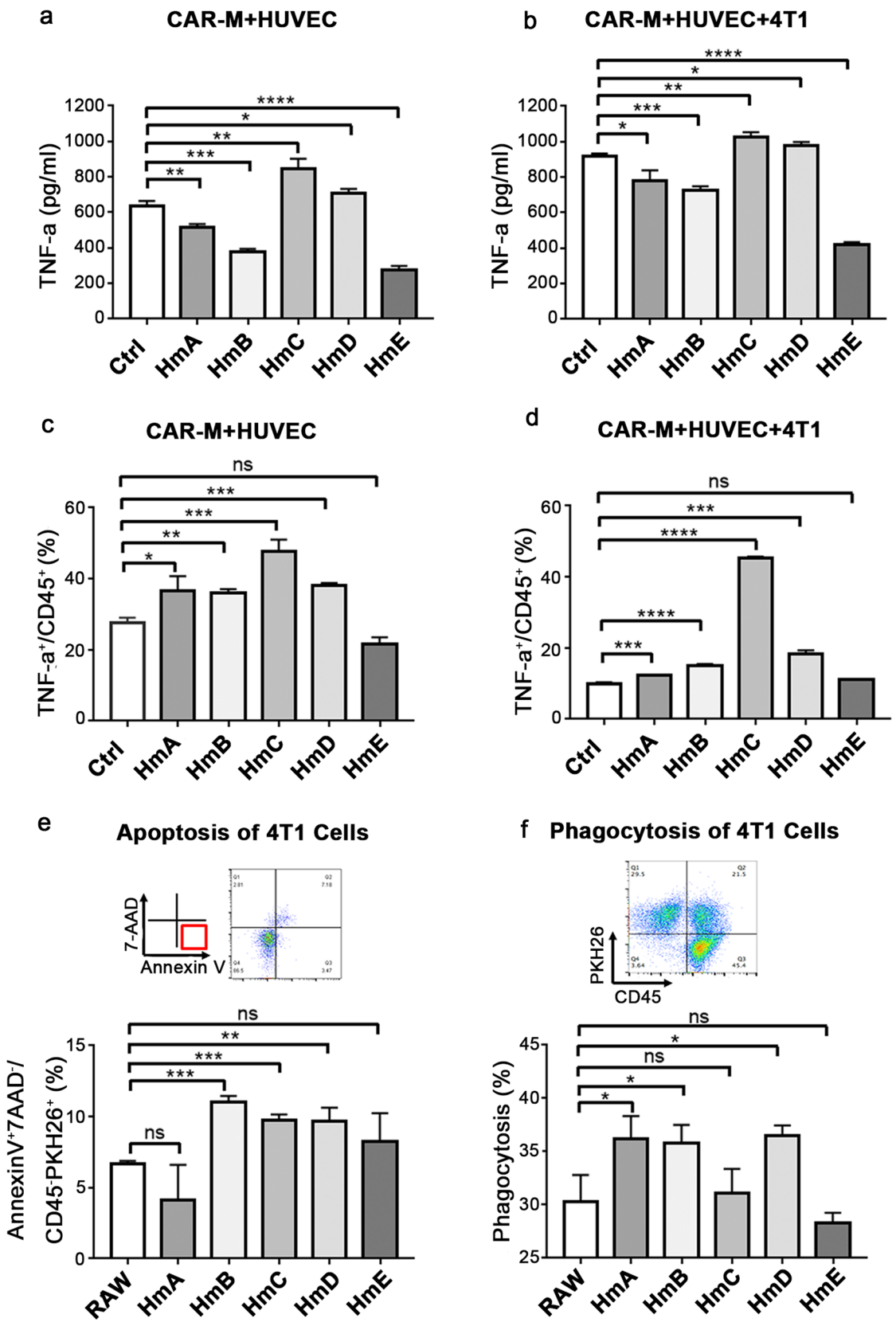
a
CAR-M+HUVEC
TNF-a (pg/ml)
Ctrl
HmA
HmB
HmC
HmD
HmE
b
CAR-M+HUVEC+4T1
TNF-a (pg/ml)
c
CAR-M+HUVEC
TNF-a+/CD45+ (%)
d
CAR-M+HUVEC+4T1
TNF-a+/CD45+ (%)
e
Apoptosis of 4T1 Cells
7-AAD
Annexin V
AnnexinV+7AAD-/
CD45-PKH26+ (%)
RAW
f
Phagocytosis of 4T1 Cells
PKH26
CD45
Phagocytosis (%)

◂**Fig.4** VEGFR2-targeting CAR-M cells can be activated by Vegfr2 to secret TNF-α. **a** Secretion of TNF-α detected by ELISA in co-culture supernatant of CAR-Ms and HUVEC cells. **b** Secretion of TNF-α detected by ELISA in co-culture supernatant of CAR-Ms, HUVEC and 4T1 cells. **c** Expression of TNF-α in CAR-Ms co-cultured with HUVEC cells by flow cytometry. **d** Expression of TNF-α in CAR-Ms co-cultured with HUVEC and 4T1 cells by flow cytometry. The incubation time was 48 h for **a-d** and 2 h for **e–f** each condition. **e** Analyze the apoptosis of 4T1 cells in co-culture model. **f** Detect phagocytosis of 4T1 cells in co-culture model. Results mean three independent repeats. ns: not significant, * $P<0.05$, ** $P<0.01$, *** $P<0.001$, **** $P<0.0001$

luciferase. Since the treatment with mmE had no obvious effect in previous experiment, it was canceled in this round. CAR-Ms was administered on day 6, day12 and day18 after tumor inoculation (Fig. 6a). The record of tumor volume depicted that treatment with mmB, mmC and mmD could slow down the growth of tumor (Fig. 6a). In terms of weight, the tumor burden was decreased in mmB and mmC group (Fig. 6b). Meanwhile, compared to control, there was no noticeable difference in the weight of organs including liver, lung and spleen of cancer-bearing mice after mmB and mmC infusion (Fig. 6c). And the weight curves of mice showed that treatment with mmB and mmC did not cause the emaciation of mice (Fig. 6d). In addition, the proportions of macrophages in the tumor of all groups were not obviously different, indicating the difference in tumor burden may not be caused by the increase in macrophages (Fig. 6e).

Furthermore, we performed the detection of macrophages in tumors using F4/80 by IHC. The result is presented in Fig. 7a. According to the quantification of data, the percentage of $F4/80^+$ area was significantly increased in the mmB and mmC group (Fig. 7c). This was consistent with the results in Fig. 6b, in which showed that the tumors in group B and group C were statistically decreased than control. It is worth emphasizing that the analysis of $F4/80^+$ cells were focused on the depths of the tumor rather than the edges or outside of the tumor. Combining with Fig. 6e, although the percentage of $CD11b^+F4/80^+$ macrophages in tumor detected by flow cytometry has no statistical difference among each group, macrophages infiltrated in the depths of tumor observed by IHC in group mmB and mmC were increased. This offers a good explanation to the shrinkage of tumor in group mmB and mmC. In addition, CD31 was detected by IHC and the quantifications were compared (Fig. 7b). The positive rate is statistically higher in mmA, mmC and mmD groups than ctrl, and a similar upward trend was observed in group B (Fig. 7d). It was indicated that although VEGFR2, the target of our CAR-Ms, was mainly expressed on vascular endothelial cells, the blood vessels marked by CD31 were not attacked by macrophages. Taken together, the results indicated that the application of mmB or mmC was effective in inhibiting tumor progression and did not exhibit significant side effects compared to the control group.

The mmC exerts antitumor effects in immunodeficient mice

Evaluation were also implemented in immunodeficient mice (Fig. 8a). It was apparent that treatment with mmC could inhibit tumor development even without the aid of adaptive immune system (Fig. 8b). Consistent with the previous results, treatment of cancer-bearing mice with mmC did not cause changes in weight of organs and bodies (Fig. 8c, d). These results demonstrated that mmC could function as the tumor suppressor even without an aid from adaptive immune cells.

Discussion

Currently, CAR-Ms have attracted growing attentions. Klichinsky et al. bound the intracellular domain of CD3 with scFv of anti-CD19, anti-mesothelin or anti-HER2 antibody to construct chimeric antigen receptors [5]. In their study, CARs delivered into macrophages via adenovirus could significantly prolonged the survival of cancer-bearing mice and reduced lung metastasis. One important mechanism is that the CAR could induce the polarization of CAR-M to M1. Zhang et al. explored an off-the-shelf CAR-Ms which came from induced pluripotent stem cells, namely CAR-iMac [7]. In their evaluation experiments, in addition to autonomic proliferation, enhanced phagocytosis and anti-tumor ability, polarization of a pro-inflammatory M1 phenotype was also an important indicator of a successful CAR-iMac.

Moreover, Mikyung et al. overcame the difficulty that immune cells had in infiltrating and targeting tumors through delivering the nanocomplexes of macrophage-targeting nanocarriers and CAR-IFN-γ-encoding plasmid to macrophages [8]. They demonstrated that successfully eliciting an M2 to M1 macrophages shift contributed to CAR-mediated tumor phagocytosis, anti-tumor immunomodulation and inhibition of solid tumor growth. All these studies inspired us to design CAR-Ms aiming at inducing M1 polarization.

LPS and IFN-γ are two typical signals inducing M1 polarization. So the receptors of LPS or IFN-γ (TLR4 or IFNGR1, IFNGR2) were applied in our chimeric antigen receptors for macrophages [12, 36]. The expression of VEGF and VEGRF2 in TME is significantly upregulated compared to normal tissues [30]. It has been shown that blocking the VEGF/VEGFR2 axis to inhibit tumor angiogenesis can be an effective tumor treatment strategy [37, 38]. So antibody against VEGFR2 was used in the design of scFv. Targeting VEGFR2 gives our CAR-Ms the potential to be applied in more than one type of tumors.

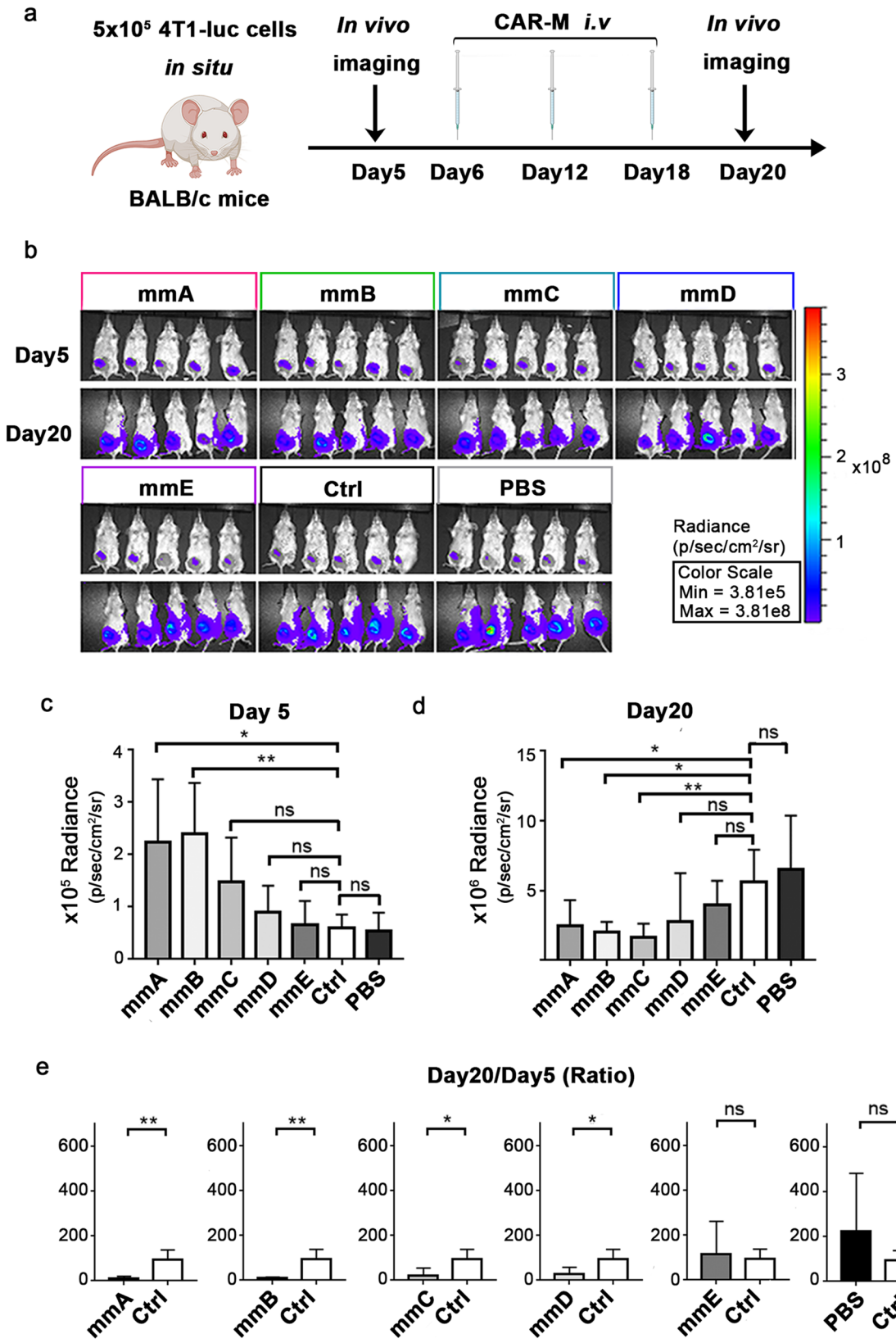

Fig.5 VEGFR2-targeting CAR-M cells, except mmE, inhibited tumor growth in 4T1-luc bearing mice model. **a** Schematic diagram of the experiment. **b** In vivo imaging of bioluminescence intensity of tumors on day 5 and day 20 after tumor inoculation. **c, d** Quantitative analysis of biofluorescence intensity on day 5 and day 20. **e** Ratio of biofluorescence intensity on day 20 to that on day 5. N = 5 mice/group. ns: not significant, * $P < 0.05$, ** $P < 0.01$

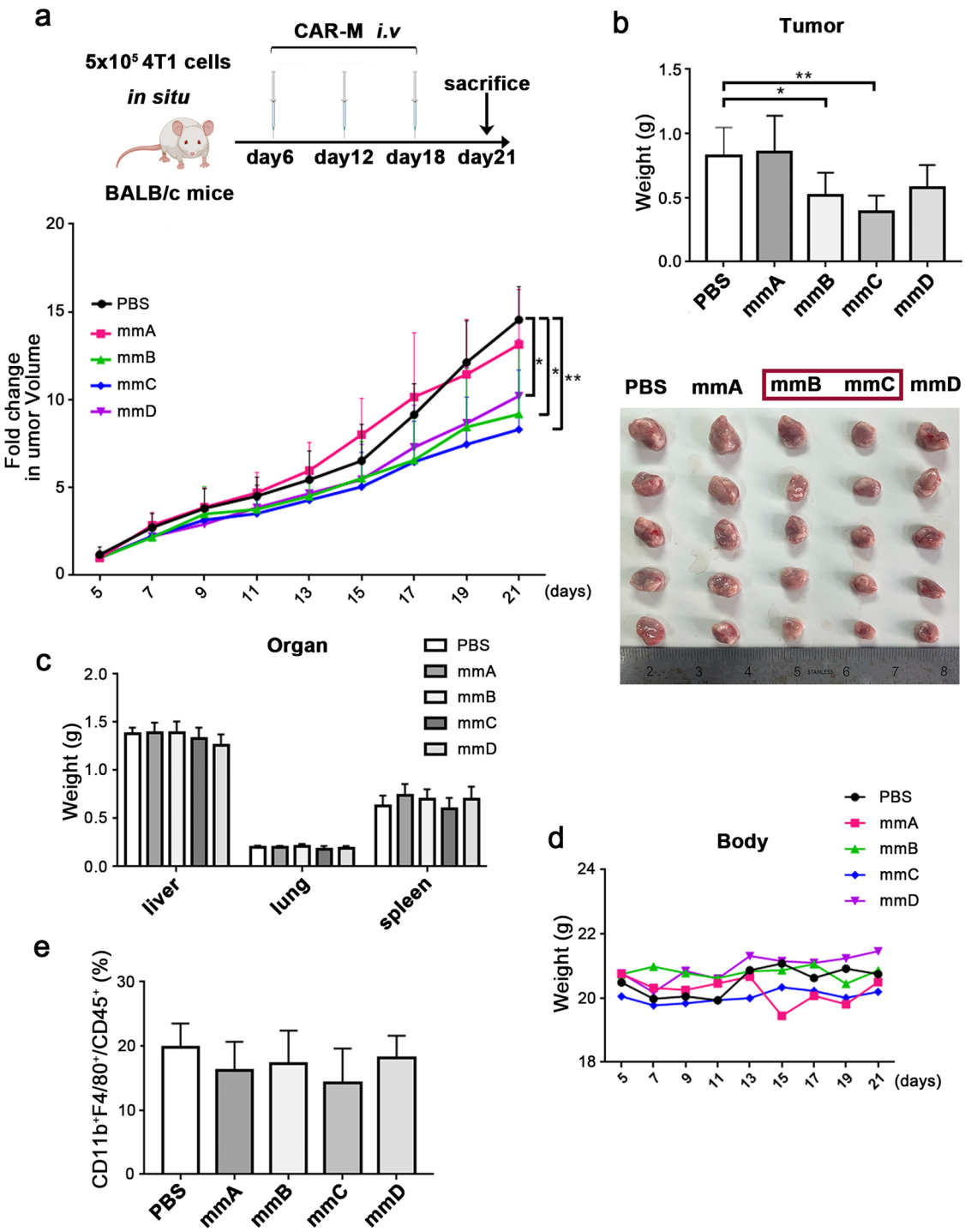

Fig.6 The mmB and mmC displayed enhanced antitumor effects in immunocompetent breast cancer mice model. **a** Schematic diagram of the experiment. **b** The weight and picture of tumors. **c** The weight of livers, lungs and spleens. **d** Body weight of tumor-bearing mice. **e** Percentage of macrophages ($CD11b^+F4/80^+/CD45^+$) in the tumor-infiltrating immune cells. N = 5 mice/group. * $P < 0.05$, ** $P < 0.01$

Given that VEGFR2 is also underexpressed on some normal cells, like hematopoietic cells, retinal progenitor cells, and neuronal cells [31], safety is a big concern when targeting it in immunotherapy. Our results showed that all five VEGFR2-targeting CAR-Ms were relatively safe because they barely phagocytosed VEGFR2-expressing 293 T cells and organs including liver, lung, spleen did not change sharply after treating tumor-bearing mice with these CAR-Ms. This could possibly be explained by following reasons: (1) Besides 'don't eat me' signals, there

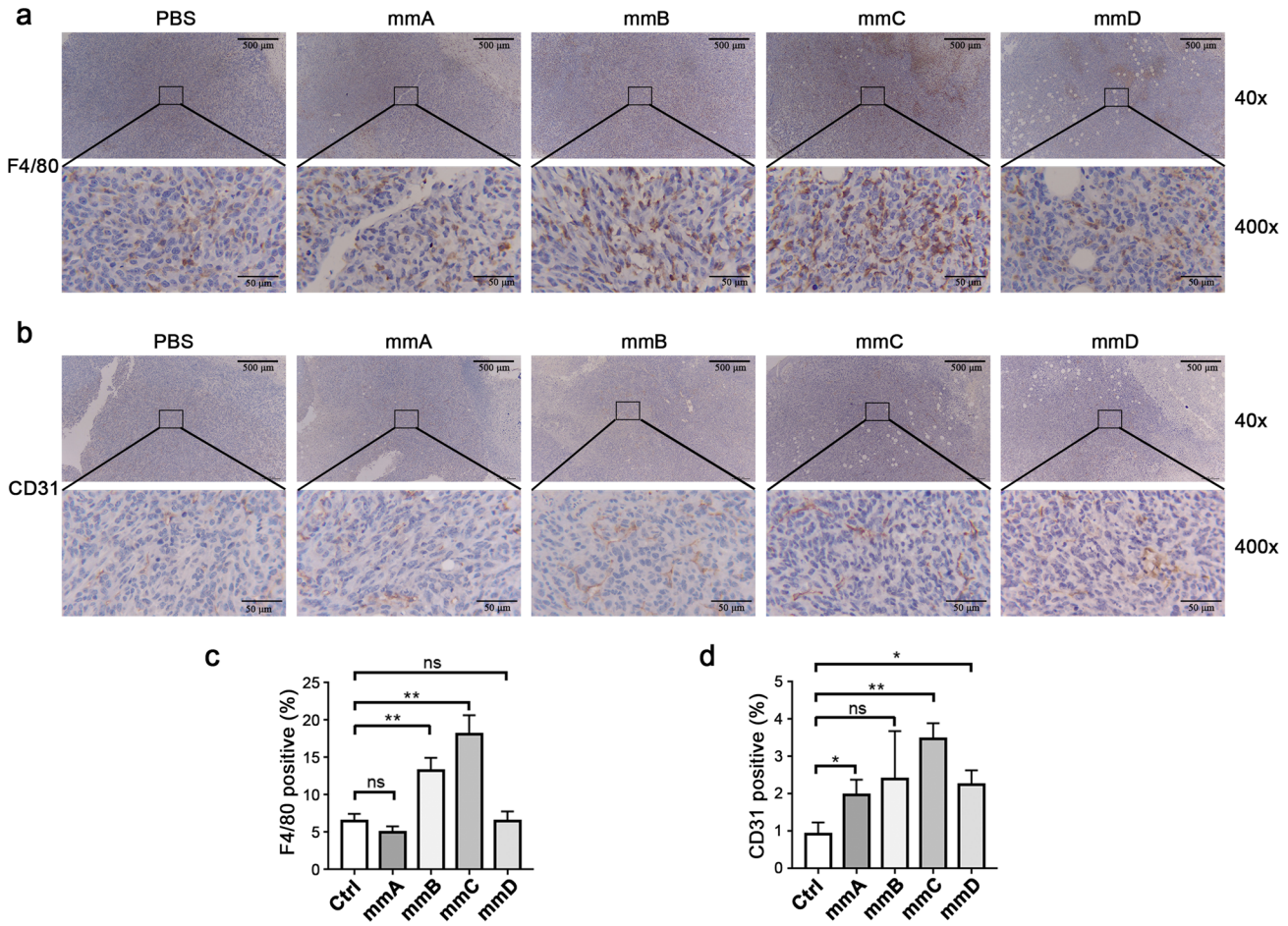

Fig.7 The mmB and mmC had an increased infiltration of macrophages and no decreased CD31 labeled blood vessels. **a** Immunohistochemical stain of F4/80. **b** Immunohistochemical stain of CD31. **c** Quantifications of F4/80. **d** Quantifications of CD31. N = 3 mice/group. * $P < 0.05$, ** $P < 0.01$

are also 'eat me' signals on tumor cells [39]. So VEGFR2-expressing endothelial cells without 'eat me' signals won't be the target for CAR-Ms to kill; (2) the design of chimeric antigen receptors is purposed to activate macrophages toward M1 polarization, while enhanced phagocytosis is not a main characterization of M1 polarization, thus, our CAR-Ms didn't directly kill non-tumor cells expressing the target gene. We also detected the TNF-α and IL-6 in the CAR-M + 293 T-mcs or CAR-M + 293 T-VEGFR2 co-culture system. The level of TNF-α produced by HmC when co-cultured with 293 T-mcs (control of 293 T-VEGFR2) was similar with the control group (Fig. S1a), but it significantly increased when co-cultured with 293 T-VEGFR2 (Fig. S1b). As for IL-6, its concentration in HmC arised from around 400 pg/ml group (Fig. S1c) when co-cultured with 293 T-mcs to nearly 600 pg/ml when co-cultured with 293 T-VEGFR2 (Fig. S1d), both of which were higher than the control group. The rise is more pronounced in HmD. It is worth mentioning that the TNF-α and IL-6 produced by RAW-264.7 were murine-derived, so they may have no direct effect on human 293 T cells.

Interestingly, MHC-II vs MHC-I, and CD86 vs CD80 showed different tendency in our results. MHC-II is predominantly expressed by professional antigen presenting cells such as dendritic cells, macrophages. It presents exogenously derived antigenic peptides mainly to $CD4^+$ T cells. MHC-I is expressed by most nucleated cells and presents endogenously derived peptide antigens mainly to $CD8^+$ T cells. Due to their structural differences, MHC-II may be able to bind a higher diversity of peptides than MHC-I, which allows increased expression of MHC-II to enhance tumor recognition by the immune system. Therefore MHC-II has a vital role in immunotherapy [40]. Forero A. et al., by analyzing 199 triple-negative breast cancer cases from the public gene expression database, confirmed the association between MHC-II pathway expression and prognosis. Elevated expression of the MHC-II pathway triggered an anti-tumor immune response, which decreased the recurrence rate of patients

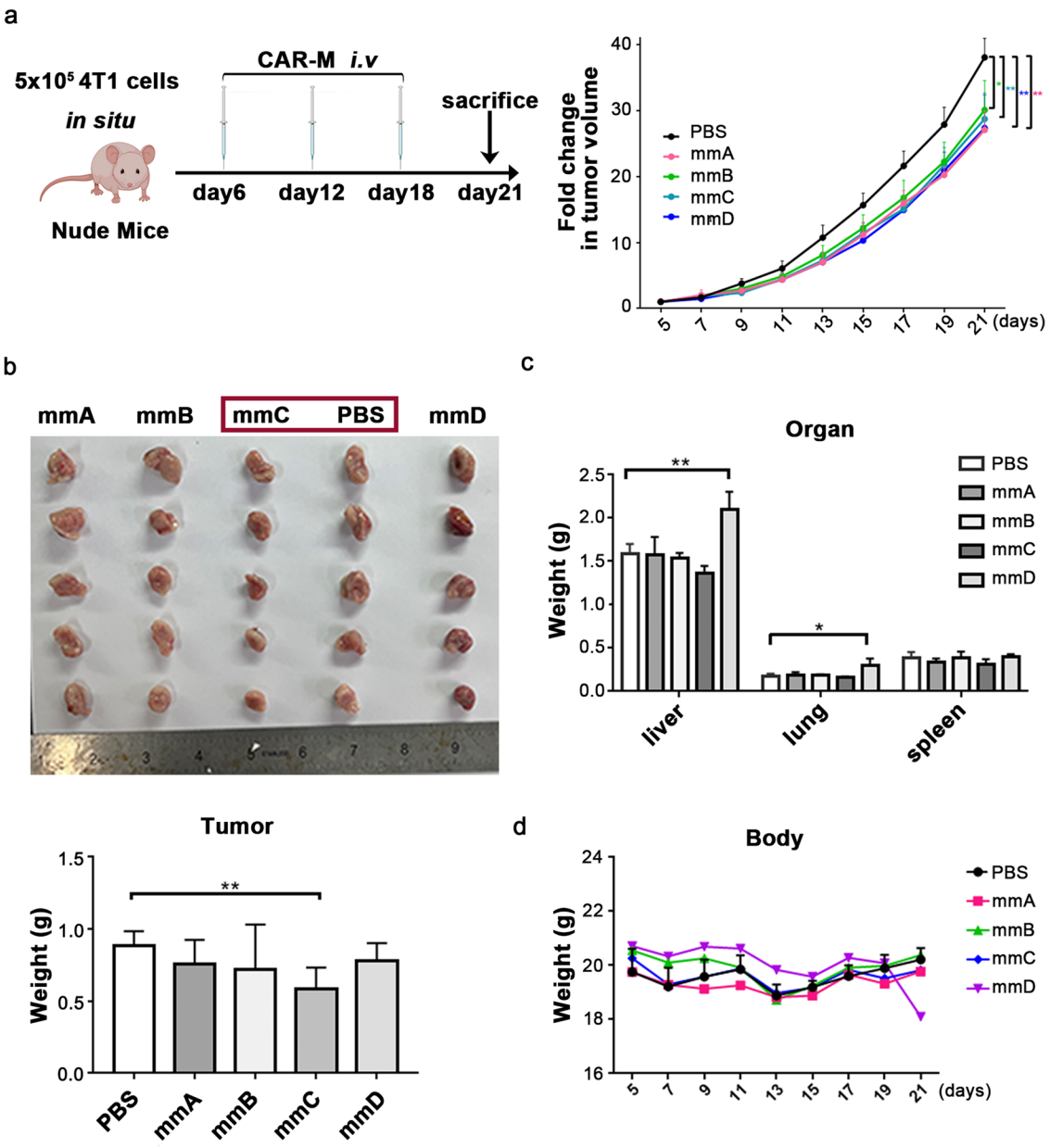

Fig.8 The mmC significantly suppressed tumor growth in breast cancer nude mice model. **a** Schematic diagram of the experiment. **b** The weight and picture of tumors. **c** The weight of livers, lungs and spleens. **d** Body weight of tumor-bearing mice. N = 5 mice/group. * $P < 0.05$, ** $P < 0.01$

[41]. CD86, a T-cell co-stimulatory molecule like CD80, had an increased expression as opposed to CD80 in our data, which was a favorable manifestation. Because CD80 binds the inhibitory receptor CTLA4 with a higher than 200-fold affinity compared to CD86, and the dissociation of the CD80-CTLA4 complex is five to eight fold slower [42]. It has been revealed that CD80 was a key ligand for CTLA4 to inhibit Th1 responses and $CD8^+$ T cell activation, while CD86 activated naive $CD4^+$ T cells and induces Th1 and Th2 responses [43]. That is to say, increased expression of MHC-II and CD86 implies enhanced positive immune function of macrophages.

TNF-α secretion by macrophages represents an acquisition of pro-inflammatory features. It induces apoptosis of tumor cells, which are associated with improved survival [17, 44]. Our results showed a significant increase in the level of TNF-α secreted by HmB-HmE, implying they had an acquisition of pro-inflammatory phenotype. Whereas mmA was unable to secrete sufficient TNF-α to trigger apoptosis, therefore mmA could not effectively induce

apoptosis of 4T1 in vitro. IL-6 is also an inflammatory factor but its role in tumor is complicated. It has been reported that IL-6 could enhance cellular invasiveness and drive tumor metastasis [45].

To summarize, we designed five CAR-Ms to promote activation through Tlr4 and/or Ifn-γ receptors. Except for HmE/mmE, the other designs including HmA/mmA, HmB/mmB, HmC/mmC, HmD/mmD more or less showed their potential in tumor inhibition in vitro. They are able to upregulate MHC-II, CD86 or Nos2 but not CD163, CD206, CD36, Arg1, secrete anti-tumor cytokine TNF-α or exert a tumor-killing effect after activated by VEGFR2 that highly expressed in the TME. The most consistent anti-tumor effect was observed in HmC/mmC, whether in vitro or in mice models. This might be explained by the simplest structure of chimeric antigen receptor in HmC/mmC, in which only intracellular of Tlr4 was inserted. As for HmE/mmE, the tandem combination of Ifngr1 and Ifngr2 without a linker may make it difficult for these receptors to form a complex, which reduced the signals passing down. Since lots of receptors, chemokines or cytokines are reported to be involved in the recruitment or regulation of macrophages and adaptive immune cells during tumor progression [9, 17], we can combine HmC/mmC and these elements to enhance the anti-tumor effects of CAR-Ms in future.

Supplementary Information The online version contains supplementary material available at https://doi.org/10.1007/s00262-023-03490-8.

Acknowledgements In the design of CAR-M, Prof Rong Xiang and Yi Shi from Nankai University have given good suggestions. Sincere acknowledgment to them for their kindly support. Elements used for Fig.2b in this article were downloaded from https://smart.servier.com. The Servier Medical Art by Servier is licensed under a Creative Commons Attribution 3.0 Unported License. This work was supported by the Prospective Research Program of the Foundation for the Development of Frontier Technology of Cell Therapy of Changzhou Xitaihu (2022-P-009, Y.L.), the Fundamental Research Funds for the Central Universities (3332022181, Z.D.) and the Bilateral Inter-Governmental S&T Cooperation Project from Ministry of Science and Technology of China (2018YFE0114300, Y.L.).

Author contributions The chimeric antigen receptors were designed by ZD and evaluated by ZL and ZD. The conditions for animal experiments were established by ZW. CC helped with the analysis and interpretation of results. The manuscript was written by ZL and edited by ZD and YL. The financial support came from funds of YL and ZD. All authors contributed to manuscript revision, read, and approved the submitted version.

Funding This work was supported by the Prospective Research Program of the Foundation for the Development of Frontier Technology of Cell Therapy of Changzhou Xitaihu (2022-P-009, Y.L.), the Fundamental Research Funds for the Central Universities (3332022181, Z.D.) and the Bilateral Inter-Governmental S&T Cooperation Project from Ministry of Science and Technology of China (2018YFE0114300, Y.L.).

Data availability The datasets generated during and/or analyzed during the current study are available from the corresponding author on reasonable request.

Declarations

Conflict of interest ZD, ZL and YL have filed a patent on the design and application of the CAR-M cells described in this project for tumor immunotherapy with National Intellectual Property Administration of China. The authors declare no other competing interests.

Ethics approval All experiments involving animals were approved by the Institute Research Ethics Committee of Peking Union Medical College (2021.9.2/ACVC-A01-2021–039) and carried out under the guidelines on laboratory animals.

References

1. Pettitt D, Arshad Z, Smith J, Stanic T, Hollander G, Brindley D (2018) CAR-T cells: a systematic review and mixed methods analysis of the clinical trial landscape. Mol Ther 26:342–353. https://doi.org/10.1016/j.ymthe.2017.10.019
2. Zhang BL, Qin DY, Mo ZM, Li Y, Wei W, Wang YS, Wang W, Wei YQ (2016) Hurdles of CAR-T cell-based cancer immunotherapy directed against solid tumors. Sci China Life Sci 59:340–348. https://doi.org/10.1007/s11427-016-5027-4
3. Bonifant CL, Jackson HJ, Brentjens RJ, Curran KJ (2016) Toxicity and management in CAR T-cell therapy. Mol Ther Oncolytics 3:16011. https://doi.org/10.1038/mto.2016.11
4. Shah NN, Fry TJ (2019) Mechanisms of resistance to CAR T cell therapy. Nat Rev Clin Oncol 16:372–385. https://doi.org/10.1038/s41571-019-0184-6
5. Klichinsky M, Ruella M, Shestova O et al (2020) Human chimeric antigen receptor macrophages for cancer immunotherapy. Nat Biotechnol 38:947–953. https://doi.org/10.1038/s41587-020-0462-y
6. Niu Z, Chen G, Chang W et al (2021) Chimeric antigen receptor-modified macrophages trigger systemic anti-tumour immunity. J Pathol 253:247–257. https://doi.org/10.1002/path.5585
7. Zhang L, Tian L, Dai X et al (2020) Pluripotent stem cell-derived CAR-macrophage cells with antigen-dependent anti-cancer cell functions. J Hematol Oncol 13:153. https://doi.org/10.1186/s13045-020-00983-2
8. Kang M, Lee SH, Kwon M et al (2021) Nanocomplex-mediated in vivo programming to chimeric antigen receptor-m1 macrophages for cancer therapy. Adv Mater 33:e2103258. https://doi.org/10.1002/adma.202103258
9. Duan Z, Luo Y (2021) Targeting macrophages in cancer immunotherapy. Signal Transduct Target Ther 6:127. https://doi.org/10.1038/s41392-021-00506-6
10. Mills CD, Kincaid K, Alt JM, Heilman MJ, Hill AM (2017) Pillars Article: M-1/M-2 macrophages and the Th1/Th2 paradigm. J. Immunol. 2000. 164: 6166–6173. J Immunol 199:2194–2201. https://doi.org/10.4049/jimmunol.1701141
11. Fitzgerald KA, Kagan JC (2020) Toll-like Receptors and the Control of Immunity. Cell 180:1044–1066. https://doi.org/10.1016/j.cell.2020.02.041

12. Lu YC, Yeh WC, Ohashi PS (2008) LPS/TLR4 signal transduction pathway. Cytokine 42:145–151. https://doi.org/10.1016/j.cyto.2008.01.006
13. Gocher AM, Workman CJ, Vignali DAA (2022) Interferon-gamma: teammate or opponent in the tumour microenvironment? Nat Rev Immunol 22:158–172. https://doi.org/10.1038/s41577-021-00566-3
14. Martinez-Sabadell A, Arenas EJ, Arribas J (2022) IFNgamma signaling in natural and therapy-induced antitumor responses. Clin Cancer Res 28:1243–1249. https://doi.org/10.1158/1078-0432.CCR-21-3226
15. Ni L, Lu J (2018) Interferon gamma in cancer immunotherapy. Cancer Med 7:4509–4516. https://doi.org/10.1002/cam4.1700
16. Ruffell B, Coussens LM (2015) Macrophages and therapeutic resistance in cancer. Cancer Cell 27:462–472. https://doi.org/10.1016/j.ccell.2015.02.015
17. Pathria P, Louis TL, Varner JA (2019) Targeting tumor-associated macrophages in cancer. Trends Immunol 40:310–327. https://doi.org/10.1016/j.it.2019.02.003
18. Anderson NR, Minutolo NG, Gill S, Klichinsky M (2021) Macrophage-based approaches for cancer immunotherapy. Cancer Res 81:1201–1208. https://doi.org/10.1158/0008-5472.CAN-20-2990
19. Gentles AJ, Newman AM, Liu CL et al (2015) The prognostic landscape of genes and infiltrating immune cells across human cancers. Nat Med 21:938–945. https://doi.org/10.1038/nm.3909
20. Chen Y, Song Y, Du W, Gong L, Chang H, Zou Z (2019) Tumor-associated macrophages: an accomplice in solid tumor progression. J Biomed Sci 26:78. https://doi.org/10.1186/s12929-019-0568-z
21. Kaneda MM, Messer KS, Ralainirina N et al (2016) PI3K gamma is a molecular switch that controls immune suppression. Nature 539:437–442. https://doi.org/10.1038/nature19834
22. Foubert P, Kaneda MM, Varner JA (2017) PI3Kgamma activates integrin alpha4 and promotes immune suppressive myeloid cell polarization during tumor progression. Cancer Immunol Res 5:957–968. https://doi.org/10.1158/2326-6066.CIR-17-0143
23. Carmeliet P (2005) Angiogenesis in life, disease and medicine. Nature 438:932–936. https://doi.org/10.1038/nature04478
24. Huang Z, Zhao B, Qin Z et al (2019) Novel dual inhibitors targeting CDK4 and VEGFR2 synergistically suppressed cancer progression and angiogenesis. Eur J Med Chem 181:111541. https://doi.org/10.1016/j.ejmech.2019.07.044
25. Apte RS, Chen DS, Ferrara N (2019) VEGF in signaling and disease: beyond discovery and development. Cell 176:1248–1264. https://doi.org/10.1016/j.cell.2019.01.021
26. Lugano R, Ramachandran M, Dimberg A (2020) Tumor angiogenesis: causes, consequences, challenges and opportunities. Cell Mol Life Sci 77:1745–1770. https://doi.org/10.1007/s00018-019-03351-7
27. De Palma M, Biziato D, Petrova TV (2017) Microenvironmental regulation of tumour angiogenesis. Nat Rev Cancer 17:457–474. https://doi.org/10.1038/nrc.2017.51
28. Tugues S, Koch S, Gualandi L, Li X, Claesson-Welsh L (2011) Vascular endothelial growth factors and receptors: anti-angiogenic therapy in the treatment of cancer. Mol Aspects Med 32:88–111. https://doi.org/10.1016/j.mam.2011.04.004
29. Ferrara N, Gerber HP, LeCouter J (2003) The biology of VEGF and its receptors. Nat Med 9:669–676. https://doi.org/10.1038/nm0603-669
30. Blagosklonny MV (2004) Antiangiogenic therapy and tumor progression. Cancer Cell 5:13–17. https://doi.org/10.1016/s1535-6108(03)00336-2
31. Melincovici CS, Bosca AB, Susman S, Marginean M, Mihu C, Istrate M, Moldovan IM, Roman AL, Mihu CM (2018) Vascular endothelial growth factor (VEGF)-key factor in normal and pathological angiogenesis. Rom J Morphol Embryol 59:455–467
32. Zheng MW, Zhang CH, Chen K et al (2016) Preclinical Evaluation of a novel orally available SRC/Raf/VEGFR2 Inhibitor, SKLB646, in the treatment of triple-negative breast cancer. Mol Cancer Ther 15:366–378. https://doi.org/10.1158/1535-7163.MCT-15-0501
33. Liu J, Lin A (2005) Role of JNK activation in apoptosis: a double-edged sword. Cell Res 15:36–42. https://doi.org/10.1038/sj.cr.7290262
34. Kapellos TS, Taylor L, Lee H, Cowley SA, James WS, Iqbal AJ, Greaves DR (2016) A novel real time imaging platform to quantify macrophage phagocytosis. Biochem Pharmacol 116:107–119. https://doi.org/10.1016/j.bcp.2016.07.011
35. Wonderling RS, Ghaffar A, Mayer EP (1996) Lipopolysaccharide-induced suppression of phagocytosis: effects on the phagocytic machinery. Immunopharmacol Immunotoxicol 18:267–289. https://doi.org/10.3109/08923979609052736
36. Ivashkiv LB (2018) IFNgamma: signalling, epigenetics and roles in immunity, metabolism, disease and cancer immunotherapy. Nat Rev Immunol 18:545–558. https://doi.org/10.1038/s41577-018-0029-z
37. Welti J, Loges S, Dimmeler S, Carmeliet P (2013) Recent molecular discoveries in angiogenesis and antiangiogenic therapies in cancer. J Clin Invest 123:3190–3200. https://doi.org/10.1172/JCI70212
38. Zhao Y, Adjei AA (2015) Targeting angiogenesis in cancer therapy: moving beyond vascular endothelial growth factor. Oncologist 20:660–673. https://doi.org/10.1634/theoncologist.2014-0465
39. Feng M, Jiang W, Kim BYS, Zhang CC, Fu YX, Weissman IL (2019) Phagocytosis checkpoints as new targets for cancer immunotherapy. Nat Rev Cancer 19:568–586. https://doi.org/10.1038/s41568-019-0183-z
40. Axelrod ML, Cook RS, Johnson DB, Balko JM (2019) Biological Consequences of MHC-II expression by tumor cells in cancer. Clin Cancer Res 25:2392–2402. https://doi.org/10.1158/1078-0432.CCR-18-3200
41. Forero A, Li YF, Chen DQ et al (2016) Expression of the MHC class ii pathway in triple-negative breast cancer tumor cells is associated with a good prognosis and infiltrating lymphocytes. Cancer Immunol Res 4:390–399. https://doi.org/10.1158/2326-6066.Cir-15-0243
42. Linsley PS, Greene JL, Brady W, Bajorath J, Ledbetter JA, Peach R (1994) Human B7–1 (CD80) and B7–2 (CD86) bind with similar avidities but distinct kinetics to CD28 and CTLA-4 receptors. Immunity 1:793–801. https://doi.org/10.1016/s1074-7613(94)80021-9
43. Lang TJ, Nguyen P, Peach R, Gause WC, Via CS (2002) In vivo CD86 blockade inhibits CD4+ T cell activation, whereas CD80 blockade potentiates CD8+ T cell activation and CTL effector function. J Immunol 168:3786–3792. https://doi.org/10.4049/jimmunol.168.8.3786
44. Kaneda MM, Messer KS, Ralainirina N et al (2016) PI3Kgamma is a molecular switch that controls immune suppression. Nature 539:437–442. https://doi.org/10.1038/nature19834
45. Jones SA, Jenkins BJ (2018) Recent insights into targeting the IL-6 cytokine family in inflammatory diseases and cancer. Nat Rev Immunol 18:773–789. https://doi.org/10.1038/s41577-018-0066-7